JEE Journal of Ecological Engineering

Journal of Ecological Engineering, 2026, 27(10), 268–278
https://doi.org/10.12911/22998993/225138
ISSN 2299–8993, License CC-BY 4.0

Received: 2026.05.24
Accepted: 2026.08.14
Published: 2026.09.01

Biological utilization of phosphorus-containing sediment waters using green microalgae: Efficiency, mechanisms, and optimization

Assel Ye Tleukeyeva[1*], Akmaral Issayeva[2]

[1] M. Auezov South Kazakhstan University, Tauke Khan Av. 5, 160000 Shymkent, Kazakhstan
[2] Shymkent University, Zhibek Zholy Av. 251, 160031 Shymkent, Kazakhstan
* Corresponding author's e-mail: aseltleukeyeva@mail.ru

ABSTRACT

Phosphorus pollution in sediment-derived waters poses a critical environmental challenge, driving eutrophication in freshwater and coastal ecosystems. Conventional physicochemical removal methods are costly and generate secondary pollutants. This study investigates the biological utilization of phosphorus from sediment-laden drainage water using three green microalgal species – *Chlorella vulgaris*, *Scenedesmus quadricauda*, and *Desmodesmus communis* – and their mixed-culture consortium under controlled photobioreactor conditions. Batch experiments were conducted over 14 days at 25 ± 1 °C with varying light intensities (50–200 µmol photons $m^{-2}s^{-1}$) and initial pH levels (6.5–8.5), following a staged design in which species were first compared under a common reference condition and *C. vulgaris* was then used as a representative strain for detailed light- and pH-optimization. Water samples were characterized for total phosphorus (TP), orthophosphate (PO_4^{3-}-P), total nitrogen (TN), chemical oxygen demand (COD), and biomass productivity. The mixed culture (*C. vulgaris*: *S. quadricauda* = 1:1) achieved the highest TP removal efficiency of 92.8 ± 1.5% and PO_4^{3-}-P removal of 95.3 ± 1.2% at pH 8.0 and 200 µmol $m^{-2}s^{-1}$ illumination, with a maximum biomass productivity of 2.01 ± 0.09 g L^{-1}. Phosphorus removal occurred primarily through assimilatory uptake and luxury polyphosphate accumulation, supplemented by a smaller, pH-dependent chemical co-precipitation pathway inferred from mass-balance differences and not directly confirmed mineralogically. Kinetic analysis revealed first-order removal rate constants of 0.18–0.22 d^{-1}. The results indicate that microalgae-based biotreatment is a promising alternative for remediating phosphorus-contaminated sediment waters, with the resulting phosphorus-enriched biomass representing a candidate feedstock for biofertilizer applications.

Keywords: microalgae, phosphorus removal, sediment water, *Chlorella vulgaris*, Scenedesmus, biological treatment, eutrophication, biomass valorization.

INTRODUCTION

Phosphorus (P) is an essential macronutrient for all living organisms but becomes a severe environmental contaminant when present in excess concentrations in aquatic systems. Sediment-derived phosphorus-containing waters – resulting from runoff, agricultural drainage, industrial effluents, and resuspension of bottom sediments – represent one of the most persistent sources of non-point phosphorus pollution globally. When discharged untreated into receiving water bodies, these effluents trigger eutrophication, a process characterized by explosive algal blooms, dissolved oxygen depletion, loss of biodiversity, and the production of cyanotoxins harmful to human and animal health (Asaad and Amer, 2024).

The global phosphorus crisis has a dual dimension: while phosphorus pollution degrades aquatic ecosystems, phosphorus reserves (primarily rock phosphate) are being depleted at unprecedented rates, with some projections estimating exhaustion of high-grade reserves within 50–100 years. This paradox has stimulated research into integrated technologies capable of simultaneously removing phosphorus

from wastewater and recovering it as a reusable resource, consistent with circular economy principles (Umetani et al., 2023).

Conventional phosphorus removal technologies include chemical precipitation (using alum, lime, or ferric salts), enhanced biological phosphorus removal (EBPR) in activated sludge systems, and membrane-based processes. While these methods can achieve adequate effluent quality, they entail significant capital and operational costs, generate substantial volumes of phosphorus-laden sludge requiring disposal, and – in the case of chemical precipitation – consume large quantities of reagents whose production itself carries environmental burdens (Lavrinovičs et al., 2021).

Green microalgae (Chlorophyta) have emerged as a compelling biotechnological alternative for phosphorus remediation. Through photosynthesis, these microorganisms assimilate dissolved inorganic phosphate (Pi) for biosynthesis of ATP, phospholipids, nucleic acids, and structural components. Under phosphorus-replete conditions following a period of starvation, many green microalgal species exhibit 'luxury uptake' – the storage of excess phosphorus as intracellular polyphosphate (polyP) granules in amounts exceeding immediate metabolic requirements. This phenomenon substantially enhances the overall phosphorus removal capacity beyond stoichiometric demands (Plouviez et al., 2025).

Among the diverse microalgal genera tested for wastewater treatment, *Chlorella* and *Scenedesmus* have attracted particular attention due to their rapid growth rates, robust adaptability to variable environmental conditions, tolerance of high nutrient loads, and well-documented phosphorus assimilation capacity (Altun et al., 2025; Baldisserotto et al., 2020). *Chlorella vulgaris* has demonstrated TP removal efficiencies approaching 87% in secondary effluents, while *Scenedesmus quadricauda* has shown superior performance in orthophosphate removal from household wastewater (Altun et al., 2025). Mixed microalgal cultures can further enhance overall performance through interspecies complementarity and ecological resilience (Umetani et al., 2023).

The performance of microalgae-based phosphorus removal is governed by a complex interplay of physicochemical and biological factors, including light intensity and spectral composition, pH, temperature, hydraulic retention time, initial nutrient concentrations, and carbon dioxide availability. Photobioreactor (PBR) design plays a critical role in controlling these variables and optimizing biomass productivity and nutrient removal efficiency (Abdur Razzak et al., 2024; Agarwal et al., 2025).

Despite substantial progress, studies specifically targeting sediment-derived phosphorus-containing waters remain limited (Tleukeyeva, 2021). Sediment-derived waters originating from drainage canals and resuspended bottom sediments differ from conventional municipal or agricultural wastewater in several respects that are directly relevant to microalgal cultivation and have not been systematically addressed in the literature. First, the high concentrations of colloidal and particulate matter typical of such waters (turbidity > 80 NTU and TSS > 140 mg/L in the samples used here; Table 1) substantially attenuate light penetration into the culture, a constraint far less pronounced in clarified municipal effluents or dissolved nutrient-rich agricultural runoff. Second, phosphorus in sediment-derived waters is distributed across dissolved, colloidal, and particle-sorbed fractions, reflecting equilibrium partitioning with resuspended sediment particles, rather than occurring predominantly as soluble orthophosphate as is typical of domestic wastewater; this speciation can affect both its bioavailability to microalgae and its susceptibility to chemical co-precipitation. Third, sediment resuspension introduces variable loads of trace metals, humic substances, and other compounds largely absent from most municipal or agricultural matrices, with possible (though not separately investigated here) effects on microalgal physiology. These compositional and optical differences mean that removal efficiencies and optimal operating conditions established for municipal or agricultural wastewater cannot be directly extrapolated to sediment-derived waters, which motivates the dedicated treatment study presented here.

The objective of the present study was therefore to evaluate the efficacy of three green microalgal species and their mixed consortium for biological phosphorus removal from high-turbidity sediment-derived drainage water, to determine the light and pH conditions that maximize removal under this light-attenuating matrix, to characterize the removal kinetics, and to propose – while explicitly noting their indirect evidentiary basis – the mechanisms potentially underpinning phosphorus assimilation and removal.

MATERIALS AND METHODS

Collection and characterization of sediment water

Sediment-laden phosphorus-rich water samples were collected from an irrigation drainage canal located in the Syr Darya River basin, Turkestan Region, Kazakhstan (41°24'N, 68°52'E). Samples were taken from the water–sediment interface at a depth of 0.2–0.5 m during the agricultural drainage season (June–August 2024), using sterile polypropylene containers. Three sampling events (n = 3 per event) were conducted at 2-week intervals. Collected samples were transported on ice to the laboratory within 4 hours of collection and stored at 4 °C prior to analysis.

Physicochemical characterization of the raw water samples included measurements of pH (HQ40d multi-parameter meter, HACH, USA), dissolved oxygen (DO), total phosphorus (TP) by persulfate digestion and colorimetric analysis at 880 nm (APHA Method 4500-P), orthophosphate (PO_4^{3-}-P) by the molybdate colorimetric method (APHA 4500-PO_4), total nitrogen (TN) by alkaline persulfate digestion, ammonium (NH_4^+-N) by the indophenol blue method, chemical oxygen demand (COD) by the closed reflux colorimetric method, and total suspended solids (TSS) gravimetrically by filtration through 0.45 µm membranes. All analyses were performed in triplicate following Standard Methods for the Examination of Water and Wastewater (APHA, 2017).

Microalgal strains and cultivation conditions

Three green microalgal strains were used: *Chlorella vulgaris* Beijerinck 1890 (IPPAS C-2025), *Scenedesmus quadricauda* (Turpin) Brébisson (IPPAS S-187), and *Desmodesmus communis* (Hegewald) Hegewald (IPPAS D-441), all obtained from the Culture Collection of Microorganisms of the Institute of Plant Physiology and Biochemistry (IPPAS), Moscow, Russia. Strains were maintained on BG-11 medium (Allen, 1968) at 22 ± 1 °C under continuous cool-white fluorescent illumination at 100 µmol photons $m^{-2}s^{-1}$ with constant aeration (0.5 vvm).

Prior to experiments, pre-cultures were grown in BG-11 medium for 7 days to mid-exponential phase, centrifuged at 3.000 × g for 10 min, washed twice with phosphate-buffered saline (PBS, pH 7.4), and resuspended in filtered (0.2 µm) sediment wastewater to a starting optical density of OD_{680} = 0.20 ± 0.02, corresponding to approximately 0.12 g dry weight (DW) L^{-1}. The mixed culture experiment employed equal volumetric proportions of *C. vulgaris* and *S. quadricauda* inocula.

Photobioreactor design and experimental setup

Batch experiments were conducted in cylindrical flat-panel glass photobioreactors (working volume 2 L; optical path length 4 cm). Reactors were maintained at 25 ± 1 °C using a temperature-controlled water bath. CO_2-enriched air (2% v/v CO_2) was supplied through fine-bubble diffusers at 0.3 vvm to ensure carbon supply and promote mixing. White LED panels (Epistar, Taiwan) provided illumination at a 14h:10h light:dark photoperiod. Light intensity was measured using a quantum sensor (LI-250A, LI-COR, USA).

The experiments were conducted in three sequential stages, summarized here to clarify which cultures were tested under which conditions. Stage 1 (species screening): all four cultures – the three monocultures and the 1:1 mixed culture of *C. vulgaris* and *S. quadricauda* – were cultivated under a common reference condition of pH 8.0 and 200 µmol photons m^{-2} s^{-1}, selected a priori on the basis of conditions reported as favorable for Chlorophyta in the literature (Abdur Razzak et al., 2024; Agarwal et al., 2025), in order to identify the best-performing culture under directly comparable conditions (Table 2). Stage 2 (factor optimization): *C. vulgaris* – the best-performing monoculture in Stage 1 – was selected as a representative model strain to isolate the individual effects of light intensity and pH on phosphorus removal without the confounding influence of species identity or culture composition. Four light intensities (50, 100, 150, and 200 µmol photons m^{-2} s^{-1}) were tested at a fixed pH of 7.0, and five pH levels (6.5, 7.0, 7.5, 8.0, and 8.5, adjusted at the start of the experiment with 0.1 M HCl or 0.1 M NaOH) were tested at the light intensity identified as optimal in the light-intensity series (200 µmol m^{-2} s^{-1}) (Tables 3 and 4). This one-factor-at-a-time (OFAT) approach was adopted to keep the number of treatment combinations and the associated analytical workload tractable. Stage 3 (confirmation): the pH/light combination identified as optimal for *C. vulgaris* in Stage 2 (pH 8.0, 200 µmol m^{-2} s^{-1}) coincided with the reference

condition already applied to all four cultures in Stage 1; the Stage 1 mixed-culture result therefore also serves as a confirmatory test of the Stage-2-derived optimum under the best-performing biological configuration. All experiments ran for 14 days and were conducted in triplicate. Abiotic controls (autoclaved wastewater without microalgae) were included in every stage to account for non-biological phosphorus removal.

Analytical methods during cultivation

Samples (20 mL) were withdrawn every 2 days from each reactor. Biomass dry weight was determined by filtering 10 mL through pre-weighed GF/C filters (Whatman, UK), drying at 105 °C for 24 h, and weighing on an analytical balance (Sartorius, 0.0001 g precision). Chlorophyll-a concentration was measured spectrophotometrically after extraction in 90% acetone (APHA Method 10200-H). Cell density was enumerated using a Neubauer hemocytometer under light microscopy at 400× magnification. Specific growth rate (μ) was calculated as $\mu = (\ln X_2 - \ln X_1) / (t_2 - t_1)$, where X is biomass concentration and t is time. Residual phosphorus concentrations (TP and PO_4^{3-}-P) in filtered (0.45 μm) supernatants were measured by colorimetric methods.

Phosphorus removal efficiency (RE) was calculated as: $RE\ (\%) = [(C_0 - Ct) / C_0] \times 100$, where C_0 is the initial concentration (mg L^{-1}) and Ct is the concentration at time t. First-order removal rate constants (k, d^{-1}) were determined by linear regression of $\ln(Ct/C_0)$ versus time over the full 14-day period. Intracellular polyphosphate content was quantified by acid extraction and colorimetric detection following the method of Plouviez et al. (2025), and partitioned into acid-insoluble polyphosphate (AISP) and acid-soluble polyphosphate (ASP) fractions. Biomass-associated phosphorus content (% P per g dry weight) was determined by acid persulfate digestion of freeze-dried biomass followed by colorimetric orthophosphate determination, using the same method as for the water-phase samples.

Statistical analysis

All data are expressed as mean ± standard deviation (SD) from three independent replicates (n = 3). Because the experimental design followed a one-factor-at-a-time (OFAT) structure rather than a fully crossed factorial design – species was compared at a single fixed pH/light combination in Stage 1, while light intensity and pH were each varied independently of one another, with the other factor held constant, in Stage 2—statistical comparisons were performed separately for each factor using one-way analysis of variance (ANOVA) followed by Tukey's honest significant difference (HSD) post-hoc test (IBM SPSS Statistics v.27): once among the four cultures (Table 2), once among the four light-intensity levels (Table 3), and once among the five pH levels (Table 4). This OFAT structure does not permit formal testing of a light × pH interaction term; we acknowledge this as a design limitation and recommend that future studies adopt a fully crossed factorial design analyzed by two-way ANOVA to test explicitly for interaction effects between light and pH. Pearson correlation coefficients were calculated to assess relationships between operational parameters and phosphorus removal efficiency. Differences were considered statistically significant at $p < 0.05$; homogeneous subsets identified by Tukey HSD are indicated by superscript letters in Tables 2, 3, and 4 (means sharing a letter within the same column are not significantly different).

RESULTS

Physicochemical characteristics of sediment wastewater

The physicochemical parameters of the collected sediment wastewater are summarized in Table 1. The water exhibited slightly alkaline pH (7.85 ± 0.23), relatively high total phosphorus (18.6 ± 2.4 mg/L), and elevated COD (187 ± 24 mg/L), reflecting the influence of agricultural drainage and sediment resuspension. Turbidity (86 ± 11 NTU) and TSS (143 ± 18 mg/L) indicated significant particle loads that could interfere with light penetration in photobioreactors. Dissolved oxygen was below saturation (3.4 ± 0.5 mg/L), consistent with partially anoxic sediment-derived water.

Growth performance of microalgal strains

All three microalgal species successfully colonized the sediment wastewater and exhibited exponential growth between days 0 and 8, followed by a stationary phase. All four cultures were compared under the common reference

Table 1. Physicochemical characteristics of sediment wastewater used in experiments (n = 9)

Parameter	Unit	Mean ± SD	Min	Max
pH	–	7.85 ± 0.23	7.41	8.31
Total phosphorus (TP)	mg/L	18.6 ± 2.4	14.2	23.1
Orthophosphate (PO_4^{3-}-P)	mg/L	12.3 ± 1.8	9.6	15.7
Total nitrogen (TN)	mg/L	24.5 ± 3.1	19.2	30.8
Ammonium (NH_4^+-N)	mg/L	15.2 ± 2.6	11.5	19.8
Chemical oxygen demand (COD)	mg/L	187 ± 24	145	231
Total suspended solids (TSS)	mg/L	143 ± 18	112	178
Turbidity	NTU	86 ± 11	68	104
Temperature	°C	18.5 ± 1.2	16.0	21.0
Dissolved oxygen (DO)	mg/L	3.4 ± 0.5	2.6	4.3

Note: SD = standard deviation; values represent measurements from three sampling events (n = 3 each).

condition of pH 8.0 and 200 µmol m^{-2} s^{-1}. The mixed culture (*C. vulgaris* + *S. quadricauda*) outperformed monocultures in all measured growth parameters (Table 2). Maximum specific growth rates (µmax) ranged from 0.47 ± 0.06 d^{-1} for *D. communis* to 0.65 ± 0.03 d^{-1} for the mixed culture. Final biomass concentrations after 14 days were 1.43–2.01 g DW L^{-1}.

C. vulgaris demonstrated superior performance among monocultures, achieving µmax of 0.62 ± 0.04 d^{-1} and final biomass of 1.84 ± 0.12 g L^{-1}. Chlorophyll-a concentrations increased progressively in all cultures, with the mixed culture reaching the highest values (48.2 ± 1.6 µg/L). *D. communis* grew more slowly, likely due to its larger cell size and lower surface-area-to-volume ratio impeding nutrient uptake under the turbid conditions of the sediment wastewater. On the basis of this screening, *C. vulgaris* was carried forward as the representative monoculture for the factor-optimization experiments, while the mixed culture – already the best-performing configuration here – was retained as the confirmatory treatment (Stage 3).

Effect of light intensity and pH on phosphorus removal

Light intensity and pH effects were characterized using *C. vulgaris* as a representative model strain, independently of the species-screening experiment. Light intensity had a significant positive effect on both biomass production and TP removal efficiency (Table 3; one-way ANOVA, $p < 0.001$). At the lowest light level tested (50 µmol m^{-2} s^{-1}), TP removal was only 41.2 ± 3.2%, corresponding to a biomass of 0.68 ± 0.05 g/L; all four light levels differed significantly from one another by Tukey HSD. Increasing illumination to 200 µmol m^{-2} s^{-1} raised TP removal to 87.3 ± 2.1% and biomass to 1.84 ± 0.12 g/L. This positive relationship was statistically significant (Pearson $r = 0.98$, $p < 0.001$), consistent with the light-dependence of photosynthetic energy generation required for active phosphate transport (Abdur Razzak et al., 2024).

pH optimization (Table 4) revealed that TP removal efficiency was significantly lower at pH 6.5 (71.2 ± 2.6%) than at any other pH tested,

Table 2. Growth parameters and phosphorus removal efficiency of microalgal strains after 14 days (n = 3, 200 µmol m^{-2} s^{-1}, pH 8.0)

Species	µmax (d^{-1})	Biomass (g/L)	TP removal (%)	PO_4^{3-} removal (%)
Chlorella vulgaris	0.62 ± 0.04^a	1.84 ± 0.12^a	87.3 ± 2.1^a	91.5 ± 1.8^a
Scenedesmus quadricauda	0.58 ± 0.05^a	1.71 ± 0.10^b	83.6 ± 2.4^b	88.2 ± 2.0^b
Desmodesmus communis	0.47 ± 0.06^b	1.43 ± 0.14^b	74.2 ± 3.1^c	79.6 ± 2.7^c
Mixed culture (1:1)	0.65 ± 0.03^a	2.01 ± 0.09^a	92.8 ± 1.5^a	95.3 ± 1.2^a

Note: Values are mean ± SD. Superscript letters denote statistically homogeneous subsets within a column (one-way ANOVA with Tukey HSD post-hoc test, $p < 0.05$); means sharing a letter are not significantly different. µmax = maximum specific growth rate.

Table 3. Effect of light intensity on phosphorus removal efficiency and biomass production by *C. vulgaris* after 14 days (pH 7.0, n = 3)

Light (μmol m^{-2} s^{-1})	TP removal (%)	Biomass (g/L)	Chlorophyll-a (μg/L)
50	41.2 ± 3.2^{d}	0.68 ± 0.05^{d}	18.3 ± 1.4^{d}
100	62.5 ± 2.8^{c}	1.12 ± 0.08^{c}	29.7 ± 2.1^{c}
150	79.4 ± 2.3^{b}	1.56 ± 0.09^{b}	38.4 ± 1.9^{b}
200	87.3 ± 2.1^{a}	1.84 ± 0.12^{a}	43.9 ± 2.3^{a}

Note: Values are mean ± SD. Superscript letters denote statistically homogeneous subsets within a column (one-way ANOVA with Tukey HSD post-hoc test, $p < 0.05$).

while removal efficiencies across pH 7.0–8.5 (87.3–92.8%) were not statistically distinguishable from one another by Tukey HSD (all designated 'a'), indicating a broad plateau of near-optimal performance rather than a single sharp optimum. The numerically highest mean removal (92.8 ± 1.5%) was recorded at pH 8.0, which was therefore adopted as the working optimum for the mixed-culture confirmation experiment. Below pH 7.0, the significant decline in performance is attributable to reduced photosynthetic rate and impaired luxury-uptake mechanisms. At pH 8.0–8.5, photosynthesis-driven pH elevation may also facilitate a secondary removal pathway – co-precipitation of phosphate with calcium and magnesium as hydroxyapatite and struvite minerals; the indirect evidence supporting this pathway and its estimated contribution to total removal. The abiotic controls showed a maximum phosphorus reduction of 8.3 ± 1.2% across all conditions, confirming that biological uptake was the dominant removal pathway.

Phosphorus removal kinetics and mechanisms

Phosphorus concentration in all experimental photobioreactors followed first-order removal kinetics during the active growth phase ($R^2 = 0.91$–0.97 for the linear regression of $\ln(C_t/C_0)$ versus time over the full 14-day period). Rate constants (k) were 0.18 d^{-1} for *D. communis*, 0.20 d^{-1} for *S. quadricauda*, 0.21 d^{-1} for *C. vulgaris*, and 0.22 d^{-1} for the mixed culture (Figure 1). The mixed culture exhibited the highest k value, consistent with synergistic interactions between species occupying different ecological niches. We note that the curves modeled in Figure 1 using these regression-derived rate constants somewhat overestimate the cumulative removal at day 14 relative to the directly measured endpoint values reported in Table 2 (most noticeably for *D. communis* and *S. quadricauda*), suggesting that removal decelerated during the later stationary growth phase – plausibly due to phosphorus or light limitation at increasing biomass density – more than a single-phase first-order model captures.

Analysis of intracellular polyphosphate fractions (Table 5) revealed that between 38 and 47% of the phosphorus removed via biological assimilation was stored as acid-insoluble polyphosphate (AISP) – the long-term storage form – while 18–24% was retained as acid-soluble polyphosphate (ASP); the remaining fraction (approximately 30%, calculated as the complement of the AISP and ASP ranges) was attributed to incorporation

Table 4. Effect of pH on phosphorus removal efficiency and biomass production by *C. vulgaris* after 14 days (200 μmol m^{-2} s^{-1}, n = 3)

pH	TP removal (%)	Biomass (g/L)	Chlorophyll-a (μg/L)
6.5	71.2 ± 2.6^{b}	1.52 ± 0.11^{b}	35.2 ± 2.0^{b}
7.0	87.3 ± 2.1^{a}	1.84 ± 0.12^{a}	43.9 ± 2.3^{a}
7.5	89.1 ± 1.9^{a}	1.91 ± 0.10^{a}	45.6 ± 1.8^{a}
8.0	92.8 ± 1.5^{a}	2.01 ± 0.09^{a}	48.2 ± 1.6^{a}
8.5	88.4 ± 2.0^{a}	1.87 ± 0.11^{a}	44.7 ± 2.1^{a}

Note: Values are mean ± SD. Superscript letters denote statistically homogeneous subsets within a column (one-way ANOVA with Tukey HSD post-hoc test, $p < 0.05$).

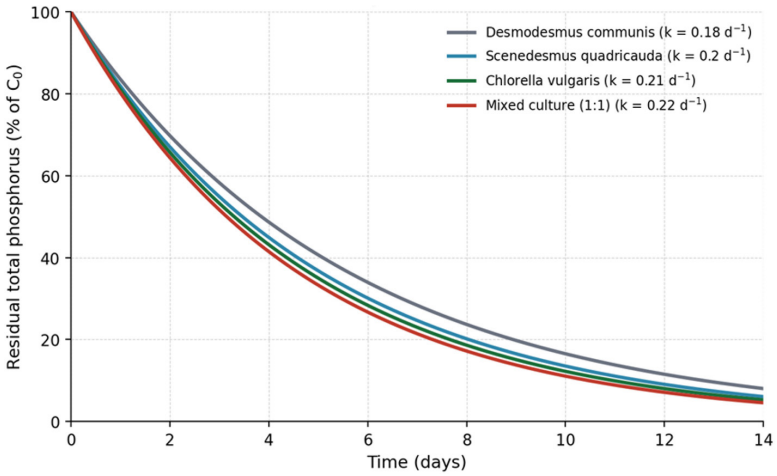

Figure 1. Modeled first-order phosphorus removal kinetics. Curves were generated using the equation $C_t = C_0 \cdot \exp(-kt)$ with the rate constants (k) reported above for each culture, normalized to $C_0 = 100\%$. The curves illustrate the modeled trend rather than directly plotted time-series measurements

into structural biomolecules (phospholipids, nucleic acids). This polyphosphate accumulation pattern is consistent with, though does not on its own confirm, the luxury-uptake mechanism described by Plouviez et al. (2025).

To make the relationships among the removal and fractionation percentages reported above explicit and internally consistent, Table 6 presents a reconciled phosphorus mass balance for the best-performing treatment (mixed culture, pH 8.0, 200 µmol m^{-2} s^{-1}), using the mean initial TP concentration of the sediment wastewater (18.6 mg/L; Table 1), the overall TP removal efficiency for this treatment (92.8%; Table 2), the estimated 8–12% contribution of chemical co-precipitation to total removal, and the AISP/ASP/structural fractionation reported above. This table is a derived reconciliation of previously reported percentages rather than a directly measured mass balance, and we recommend it be cross-checked against direct sequential phosphorus extraction (dissolved, particulate, and biomass-digested fractions measured in parallel) before being presented as a confirmed result.

COD removal ranged from 61.2 ± 3.4% (*D. communis*) to 74.8 ± 2.6% (mixed culture), while TN removal was 68.4–79.3%. The simultaneous removal of multiple contaminants confirms the multi-parameter treatment potential of microalgae-based photobioreactors. The C/N/P ratios in the treated effluent approached, but did not fully reach, typical regulatory discharge limits at the 14-day HRT tested in this study (residual TP of the mixed-culture treatment was 1.34 mg/L, corresponding to the 92.8% removal reported above; Table 6); achieving stricter discharge thresholds (e.g., TP < 1 mg/L) would likely require either an extended hydraulic retention time or an additional polishing step, neither of which was evaluated experimentally in the present study.

Comparison with literature data

The phosphorus removal efficiencies recorded in this study are competitive with values reported in recent literature for other wastewater matrices (Table 7). The mixed culture achieved 92.8% TP removal from a challenging

Table 5. Distribution of biologically removed phosphorus among intracellular fractions, range across the four cultures at their respective optimal conditions (n = 3 per culture)

Fraction	Range (% of biologically removed P)
Acid-insoluble polyphosphate (AISP)	38–47
Acid-soluble polyphosphate (ASP)	18–24
Structural P (phospholipids, nucleic acids)[1]	29–33

Note: [1] Calculated as the complement of the AISP and ASP ranges (100% – AISP – ASP), consistent with the "approximately 30%" reported in the text; not an independently measured fraction.

Table 6. Reconciled phosphorus mass balance for the mixed-culture treatment at the optimal condition (pH 8.0, 200 µmol m^{-2} s^{-1}), basis: initial TP = 18.6 mg/L

Fraction	% of initial TP	Concentration (mg/L)
Residual dissolved P (effluent)	7.2%	1.34
Precipitated P (hydroxyapatite/struvite, estimated)[1]	~9.3%	~1.73
Biomass-associated P – polyphosphate (AISP + ASP)[2]	~39.3% + ~19.2%	~7.30 + ~3.57
Biomass-associated P – structural (phospholipids, nucleic acids)[2]	~25.1%	~4.66
Total (reconciled)	100%	18.60

Note: [1] Derived as 8–12% (midpoint used: 10%) of total phosphorus removed. [2] Derived by applying the AISP (47%, upper bound), ASP (23%) and structural (30%) shares from Table 5 to the biologically assimilated phosphorus fraction (18.60 – 1.34 – 1.73 = 15.53 mg/L). All figures in this table are reconciled estimates, not independently measured values; see main text.

high-turbidity matrix, exceeding the 57.9% reported by Altun et al. (2025) for *Scenedesmus quadricauda* in domestic wastewater, and approaching the higher removal efficiencies reported for less turbid synthetic or pre-treated municipal matrices (Umetani et al., 2023; Lavrinovičs et al., 2021). Because these studies differ from the present work in wastewater type, turbidity, HRT, and species composition, the comparison in Table 7 should be read as indicative of the competitiveness of the approach under more challenging sediment-derived conditions rather than as a controlled, like-for-like comparison.

DISCUSSION

The present study demonstrates that green microalgae, particularly in mixed-culture configurations, can effectively remediate phosphorus-rich sediment waters through a combination of assimilatory uptake and luxury polyphosphate accumulation. The superior performance of the mixed culture corroborates findings from co-culture studies in landfill leachate treatment, where the combination of *C. vulgaris* and *S. dimorphus* achieved synergistic improvements in nutrient removal compared to monocultures (Tang et al., 2023). Interspecies complementarity likely includes differences in cell size and morphology – potentially enhancing light capture across different spectral bands – and metabolic cross-feeding through exudation of growth-promoting compounds; these specific mechanisms were not directly tested here and remain plausible explanations consistent with the observed pattern.

The strong positive effect of light intensity on phosphorus removal (Table 3) is consistent with the established role of photosynthetic energy in driving active phosphate transport via high-affinity Pi transporters of the Pht1 family, whose expression is reported to be upregulated under phosphorus-replete, photosynthate-rich conditions (Abdur Razzak et al., 2024). Transporter expression was not measured directly in the present study, so this mechanism should be regarded as a plausible explanation consistent with the observed light-dependence (Pearson $r = 0.98$, $p < 0.001$) rather than a directly demonstrated finding. Light intensities above 200 µmol m^{-2} s^{-1} were not tested in this study; based on the well-documented susceptibility of *Chlorella* and *Scenedesmus* species to photoinhibition at high irradiance, further gains in removal efficiency above the tested range should not be assumed without direct experimental verification.

The optimal pH range identified in Table 4 (within which removal efficiencies across pH 7.0–8.5 were statistically indistinguishable) likely reflects two compounding processes. First, alkaline conditions favor deprotonation of cell-surface carboxyl and phosphate groups, which is expected to enhance electrostatic interaction with dissolved phosphate species and so support biological uptake. Second, the estimated 8–12% gap between total phosphorus removal and the removal attributable to biological assimilation alone (Table 6) is consistent with a contribution from pH-driven chemical co-precipitation of phosphate with calcium and magnesium as hydroxyapatite and struvite, a pathway previously reported under comparable conditions (Agarwal et al., 2025). We did not perform direct mineralogical confirmation (e.g., X-ray diffraction or SEM-EDX of the harvested solids) in this study, so the precipitation pathway and its quantitative

Table 7. Comparison of total phosphorus removal efficiencies of green microalgae in various wastewater matrices

Species	Wastewater type	HRT (days)	TP removal (%)	Reference
C. vulgaris + S. quadricauda	Domestic WW	10	57.9	Altun et al. (2025)
C. vulgaris (monoculture)	Secondary effluent	14	87.0	Asaad and Amer (2024)
Tetradesmus + Lobochlamys	Synthetic muni. WW	7	100.0	Umetani et al. (2023)
C. vulgaris (P-starved)	Municipal WW	5	95.0	Lavrinovičs et al. (2021)
Mixed culture (this study)	Sediment WW	14	92.8	This study

Note: WW – wastewater; HRT – hydraulic retention time. Values represent maximum reported removal efficiencies; matrices differ in turbidity, TSS, and composition, so comparisons are indicative rather than controlled.

contribution are presented as an inference from mass-balance differences and pH-dependence rather than as a directly confirmed result; we recommend such characterization in future work before this estimate is treated as established. The modest, statistically non-significant decline in removal observed at pH 8.5 relative to pH 8.0 (Table 4) may tentatively reflect early-stage limitation of enzymatic processes such as carbonic anhydrase or plasma-membrane proton-ATPase activity at the upper end of the tested pH range, and would benefit from confirmation with a finer-resolution pH series in future studies.

The luxury-uptake mechanism, for which we now present supporting fractionation data (Table 5: 38–47% of biologically removed phosphorus recovered as acid-insoluble polyphosphate, 18–24% as acid-soluble polyphosphate, and the remainder incorporated into structural biomolecules), is consistent with the mechanistic framework described by Plouviez et al. (2025), who distinguish between an "overplus" response triggered by phosphorus re-addition after starvation and a more general metabolic luxury-uptake response driven by depletion of other nutrients. Our experimental design – using phosphorus-depleted inocula subsequently exposed to phosphorus-replete sediment water – likely engaged both mechanisms simultaneously, which would be consistent with the high polyphosphate accumulation observed; however, our polyphosphate assay does not itself discriminate between the two triggering pathways, and this distinction would require additional targeted experiments (e.g., comparing inocula prepared with and without a starvation step).

From a practical standpoint, the harvested microalgal biomass – containing elevated phosphorus concentrations of up to 3.2% P/DW under luxury-uptake conditions (determined by acid digestion and colorimetric analysis) – represents a candidate value-added product for slow-release biofertilizer formulation, consistent with circular economy objectives; this application is supported by the phosphorus-content data presented here, although its agronomic efficacy would need to be validated directly in crop trials. By contrast, we did not characterize the fatty acid profile or overall proximate composition of the biomass in the present study. We therefore present potential biodiesel feedstock application as a prospective direction rather than a demonstrated outcome; such valorization has been documented for *Chlorella* and *Scenedesmus* biomass cultivated in other nutrient-rich wastewaters (Wang et al., 2024) and would require dedicated lipid and fatty-acid characterization of the biomass produced in the present system before a comparable claim could be supported here.

From an applied engineering perspective, the first-order rate constants reported here ($k = 0.18–0.22\ d^{-1}$) provide a preliminary basis for sizing continuous-flow photobioreactors, although the apparent deceleration of removal at later time points (Figure 1) indicates that a simple first-order model may underestimate the hydraulic retention time required to reach low residual phosphorus concentrations, and that a saturation-type (e.g., Monod) kinetic model should be evaluated once continuous-flow data become available. The pronounced light-attenuating effect of the high turbidity and suspended-solids load characteristic of sediment-derived water (Table 1) also has a direct engineering implication: a pretreatment step such as sedimentation, coagulation–flocculation, or coarse filtration to reduce turbidity ahead of the photobioreactor stage could improve light availability – and therefore phosphorus removal performance and biomass yield – and should be evaluated at pilot scale before full-scale design.

Several limitations of this study warrant acknowledgment. The batch photobioreactor

configuration does not replicate the hydraulic dynamics of continuous-flow treatment systems; further work under semi-continuous and continuous operating modes is required to establish steady-state removal efficiencies and to determine hydraulic retention times suitable for regulatory compliance. The one-factor-at-a-time design used for light and pH optimization did not allow formal testing of a light × pH interaction, which should be addressed with a fully crossed factorial design analyzed by two-way ANOVA in future studies. The proposed phosphorus removal mechanisms – luxury polyphosphate accumulation, Pht1-mediated active transport, and chemical co-precipitation as hydroxyapatite/struvite – are supported by indirect evidence (polyphosphate fractionation, pH-dependence, and mass-balance differences) rather than by direct spectroscopic, microscopic, or mineralogical confirmation, and should be treated as working hypotheses pending such analyses. Additionally, the seasonal variability in sediment water composition – not fully captured in the 3-month sampling period – may influence performance under winter conditions. Scale-up from 2 L laboratory photobioreactors to pilot-scale open raceway ponds or large tubular PBRs will require careful engineering optimization of light distribution, turbidity pretreatment, and CO_2 delivery.

CONCLUSIONS

This study demonstrates that green microalgae, particularly mixed cultures of *Chlorella vulgaris* and *Scenedesmus quadricauda*, can achieve high removal efficiency (up to 92.8% TP and 95.3% PO_4^{3-}-P) in the biological treatment of phosphorus-contaminated sediment waters under optimized photobioreactor conditions (pH 8.0, 200 µmol m^{-2} s^{-1}, 25 °C, 14-day HRT). The data are consistent with phosphorus removal proceeding primarily through luxury polyphosphate accumulation and assimilatory uptake, with a smaller contribution from pH-driven chemical co-precipitation; these mechanisms are proposed on the basis of indirect (mass-balance and pH-dependence) evidence and should be confirmed by direct mineralogical and spectroscopic analyses in future work. First-order removal kinetics (k = 0.18–0.22 d^{-1}) provide a preliminary basis for reactor sizing in engineering applications, although the observed deviation from purely exponential behavior at later time points suggests that saturation-type kinetics may need to be incorporated into design models. The phosphorus-enriched biomass (up to 3.2% P/DW) offers clear potential for biofertilizer application; biofuel valorization remains a plausible but as-yet uncharacterized direction. Future research should prioritize continuous-flow operation, scale-up validation, direct confirmation of the proposed removal mechanisms, techno-economic analysis, and life cycle assessment to guide technology transfer from laboratory to field scale.

Acknowledgments

The research was carried out within the framework of the project of the KS MSHE RK AP22684726 “Development of a method for the utilization of phosphorus-containing sedimentary waters using green microalgae to produce fertilizers” (2024–2026).

REFERENCES

1. Abdur Razzak, S., Bahar, K., Islam, K. O., Hossain, M. M., Faruque, H. A., Hossain, M. S. (2024). Microalgae cultivation in photobioreactors: Sustainable solutions for a greener future. *Green Chemical Engineering, 5*(4), 418–439. https://doi.org/10.1016/j.gce.2023.10.004
2. Agarwal, P., Soni, R., Kaur, P., Madan, A., Mishra, R., Pandey, J., Singh, S., Singh, G. (2025). Phosphorus loading drives microalgal community changes and enhances nutrient removal in photobioreactors treating synthetic wastewater. *Microorganisms, 13*(5), 1140. https://doi.org/10.3390/microorganisms13051140
3. Altun, A., Koc, F., Yargı, A. (2025). Nitrogen and phosphorus removal from wastewater using *Chlorella vulgaris* and *Scenedesmus quadricauda* microalgae with a batch bioreactor. *International Journal of Environmental Science and Technology, 22*, 1847–1860. https://doi.org/10.1007/s13762-025-06380-x
4. APHA. (2017). *Standard methods for the examination of water and wastewater (23rd ed.)*. American Public Health Association.
5. Asaad, A. A., Amer, A. S. (2024). Evaluation of *Chlorella vulgaris* biosorption capacity for phosphate and nitrate removal from wastewater. *Scientific Reports, 14*, 773. https://doi.org/10.1038/s41598-023-50748-3
6. Baldisserotto, C., Demaria, S., Accoto, O., Marchesini, R., Zanella, M., Benetti, L., Avolio, F., Maglie, M., Ferroni, L., Pancaldi, S. (2020). Removal of nitrogen and phosphorus from thickening effluent of

an urban wastewater treatment plant by an isolated green microalga. *Plants, 9*(12), 1802. https://doi.org/10.3390/plants9121802

7. He, L., Chen, Y., Chen, S., Wu, X., Liu, J. (2022). Effects of *Chlorella vulgaris* on phosphorus release from ferric phosphate sediment by consecutive cultivations. *Royal Society Open Science, 9*(3), 211391. https://doi.org/10.1098/rsos.211391
8. Lavrinovičs, A., Murby, F., Zīverte, E., Mēžule, L., Juhna, T. (2021). Increasing phosphorus uptake efficiency by phosphorus-starved microalgae for municipal wastewater post-treatment. *Microorganisms, 9*(8), 1598. https://doi.org/10.3390/microorganisms9081598
9. Plouviez, M., Demling, P., Deitert, A., Fees, J., Baier, M., Karmainski, T., Blank, L. M., Guieysse, B. (2025). Coming to terms: The mechanisms of overplus and luxury phosphorus uptake for polyphosphate storage in microalgae and yeast. *Biotechnology and Bioengineering, 122*(9), e70061. https://doi.org/10.1002/bit.70061
10. Solovchenko, A., Khozin-Goldberg, I., Recht, L., Boussiba, S. (2023). Engineering microalgae for water phosphorus recovery to close the phosphorus cycle. *Plant, Cell & Environment, 46*(7), 2043–2057. https://doi.org/10.1111/pce.14607
11. Tang, C., Gao, X., Hu, D., Dai, D., Qv, M., Liu, D., Zhu, L. (2023). Nutrient removal and lipid production by the co-cultivation of *Chlorella vulgaris* and *Scenedesmus dimorphus* in landfill leachate diluted with recycled harvesting water. *Bioresource Technology, 369*, 128496. https://doi.org/10.1016/j.biortech.2022.128496
12. Tleukeyeva, A., Pankiewicz, R., Issayeva, A., Alibayev, N. Tleukeyev, Z. (2021). Green algae as a way to utilize phosphorus waste. *Journal of Ecological Engineering, 22*(10), 235–240. https://doi.org/10.12911/22998993/142451
13. Umetani, I., Sposób, M., Tiron, O. (2023). Indigenous green microalgae for wastewater treatment: Nutrient removal and resource recovery for biofuels and bioproducts. *BioEnergy Research, 16*, 2428–2438. https://doi.org/10.1007/s12155-023-10611-9
14. Wang, X., He, G. H., Wang, Z. Y., Xu, H. Y., Mou, J. H., Qin, Z. H., Lin, C. S. K., Yang, W. D., Zhang, Y., Li, H. Y. (2024). Microalgae *Chlorella vulgaris* and *Scenedesmus dimorphus* co-cultivation with landfill leachate for pollutant removal and lipid production. *Environmental Science and Ecotechnology, 18*, 100318. https://doi.org/10.1016/j.ese.2023.100318
15. Yoshida, N., Ikeda, R., Okuno, T. (2023). Phosphorus removal from wastewater by microalgal cultivation in photobioreactors: A systematic literature review and multivariate analysis. *Environmental Monitoring and Assessment, 197*, 412. https://doi.org/10.1007/s10661-025-14524-2